ACS Catalysis

Research Article

pubs.acs.org/acscatalysis

Catalyst Inefficiencies: Supported Ring-Opening Metathesis Polymerization Catalyst Yields Its Ensemble Rate from a Small Number of Molecular Active Sites

Quinn T. Easter, Vanessa Trauschke, and Suzanne A. Blum*

Department of Chemistry, University of California, Irvine, Irvine, California 92697-2025, United States

Supporting Information

ABSTRACT: A supported ruthenium metathesis catalyst misleadingly appears efficient on the basis of ensemble rate data. Nonaveraged single-particle microscopy studies described herein reveal a significant interparticle and intraparticle reactivity heterogeneity and a potential of increasing catalytic efficiency. These SEM, EDS, and optical microscopy studies of ring-opening metathesis polymerization establish a mechanism for this spatial distribution in which most of the molecular ruthenium centers are catalytically inactive. Further, the morphology of the growing polynorbornene arises from its synthesis at individual catalytically active regions. These results suggest an expanded role for single-particle microscopy in detecting spatial reactivity heterogeneity and mechanisms of polymer morphology formation, even in such "large" systems of ~10^{15} immobilized molecular complexes, and in employing this detected heterogeneity to identify and implement specific methods for improving catalysts.

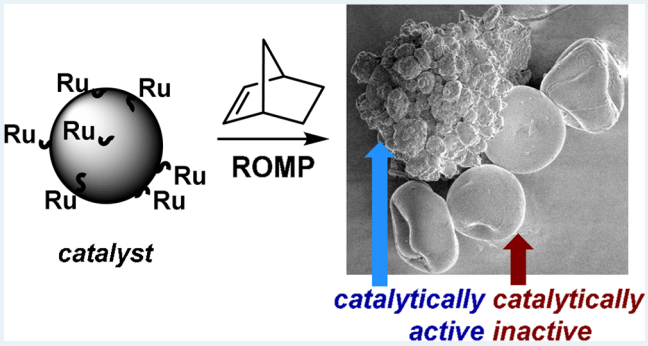

KEYWORDS: *single particle, microscopy, catalysis, spatial heterogeneity, polymerization*

INTRODUCTION

Supported molecular catalysts have the advantage of facilitating separations and recyclability and limiting reactor fouling while in theory retaining some of the uniformity of the environment around the active metal center possessed by homogeneous molecular catalysis.[1] This uniformity of chemical environment has led to supported catalysts being termed "well-defined".[2] Nevertheless, immobilized catalysts can retain the original or display reactivity[3] that is different from their otherwise analogous soluble molecular congeners because of differences in the local environment created by the support.[4] In part, the difficulty in characterizing these systems arises from the measurement challenge of characterizing the reactivity distributions that are obscured by ensemble averaging in traditional bulk measurements.

Herein, we describe optical and SEM microscopy studies of the interparticle and intraparticle reactivity heterogeneity of single resin beads[5−19] of a supported molecular Grubbs−Hoveyda-type ruthenium metathesis catalyst[2] during the polymerization of norbornene (eq 1). This supported catalyst system was chosen for studies because of its commercial availability and the industrial importance of polynorbornene produced by ruthenium-catalyzed ring-opening metathesis polymerization.[20] We also examine an ongoing mechanistic debate over the nature of the initiation distribution of the homogeneous version of this catalyst.[21−25] This distribution is obscured by ensemble averaging in traditional measurements, and in this vein, we highlight both the potential and the limitations of using single-particle techniques to address this question via supported versions of the catalyst.

Polymerization of norbornene by this catalyst is complete in about an hour at ambient temperature with a starting concentration of 1.4 M monomer and 0.08 mol % Ru. Given this short reaction time under mild conditions and low catalyst loading, the catalyst misleadingly appears efficient and already optimized when examined on this bulk reaction scale.

In this system, ruthenium carbene catalysts are supported on proprietary resin beads of ~125 μm in diameter and, at 0.5 mmol/g loading of ruthenium, contain ~10^{15} potentially active "well-defined" molecular metal catalyst complexes per resin support bead. We show the surprising result that in these large systems of 10^{15} chemically well-defined[2] complexes, the traditional ensemble-averaged reactivity data obscures an underlying tremendous distribution of catalytic reactivity[26−29] and potential for catalyst optimization.

The major findings of these studies are (1) over 70% of the support beads are fully inactive to the detection limits of the methods and lack active sites that contribute significantly to the generation of the polynorbornene; (2) on the active beads, the majority of polymer forms at only a small number of locations;

Received: January 11, 2015
Revised: February 28, 2015
Published: March 2, 2015

DOI: 10.1021/acscatal.5b00046
ACS Catal. 2015, 5, 2290−2295

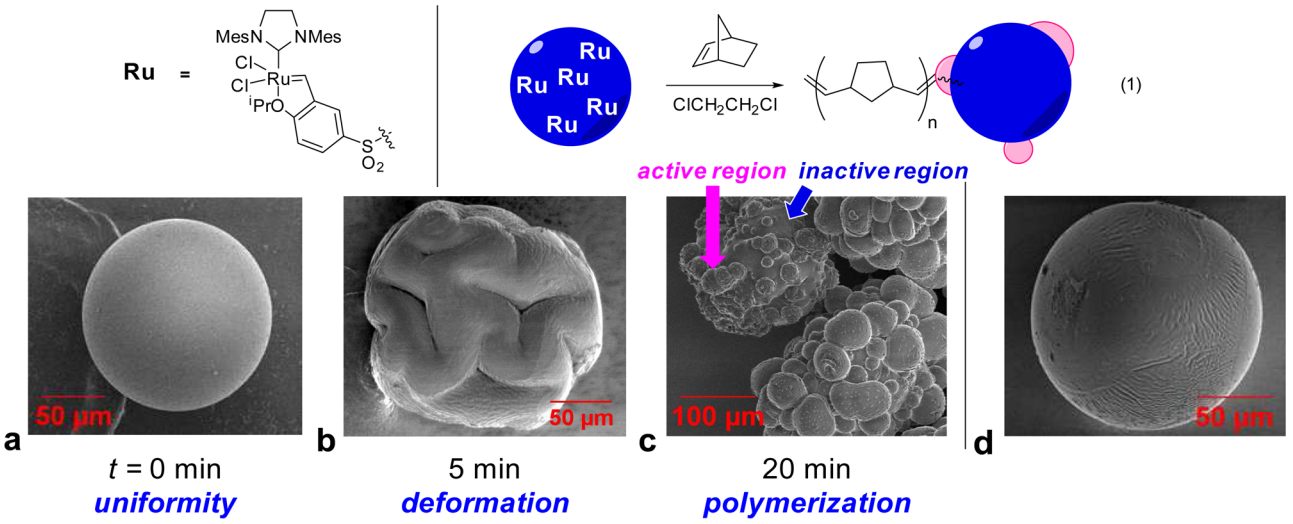

Figure 1. Three distinct time regimes of reactivity, shown by SEM images obtained at different time points in the polymerization reaction. (a) Uniformity. Image of the bead at 0 min, showing the homogeneity of the bead surface. (b) Deformation and dimpling of beads that was observed only in the presence of DCE and monomer. (c) Polymerization from specific locations while others remained inactive; polymerization observed as hemispherical protrusions on the surface of the bead at 20 min as a moderately active bead (upper left) and a highly active bead (lower right). (d) Control: representative catalyst bead in the presence of DCE solvent, but in the absence of monomer, does not show the dimpling or deformation that occurs in the presence of monomer.

(3) the ruthenium is more evenly distributed across and within a catalyst bead than is distributed the catalytic reactivity; (4) polymer morphology is influenced by its growth from individual locations; and (5) this microscale, heterogeneous spatial reactivity suggests an untapped potential for increasing catalyst efficiency in this commercial system that was previously unrecognized. Tapping into this potential lead to improving the catalytic efficiency by mechanically pressing the beads to deform them prior to the reaction.

RESULTS AND DISCUSSION

Scanning Electron Microscopy. SEM studies revealed three distinct catalytic time regimes. First, at t = 0 min, the resin-supported catalyst beads were uniformly sized, uniformly spherical, and nearly featureless (t = 0 min; Figure 1a). This SEM micrograph was obtained on a sample of the beads as received directly from the manufacturer without exposure to solvent or monomer.

The second regime was observed after addition of 1,2-dichloroethane (DCE), an efficient solvent for olefin metathesis,[30] and norbornene monomer initiated the polymerization reaction. This catalysis produced a divergence of the topology of the beads that was uniquely discernible by microscopy techniques; beads exposed to DCE in the absence of monomer did not show a similar topology divergence (Figure 1d). An initial deformation period consistent with an induction period involving the support[31] lasted ∼5 min, during which all of the beads dimpled and deformed, as detected by SEM (Figure 1b). More than half of all beads stalled at this deformation stage and did not progress to the third stage.

The third regime occurred after 5 min, wherein only some of the dimpled beads then exhibited spatially heterogeneous catalytic polymerization reactivity (20 min; Figure 1c). During this time regime, polymerization occurred from less than half of the beads and only from specific loci on those active beads, demonstrating both interparticle and intraparticle reactivity heterogeneity. The polynorbornene produced in this system, confirmed by Raman spectroscopy,[32] was sufficiently insoluble to remain attached to the beads during the full course of the polymerization reaction. This polymer growth was observed as hemispherical protrusions on the surface of the beads by SEM. The location of the regions growing polynorbornene pinpointed the loci of catalytic reactivity.

Polymer Morphology. With the microscopy-generated understanding that the final bulk polymer was synthesized by a small number of active loci, we next examined the morphology of the polynorborene formed at these individual loci. The morphology of polymers influences their useful properties, such as optical transparency, conductivity, and thermal stability, and depends strongly on the nature of the catalyst support.[4] In most cases, the morphology of the nascent polymer displayed a defined repeating pattern (Figure 2b); this pattern was a spiral of well-defined ridges with repeating units of ∼3 μm. This pattern spread to longer distances with increased polymer growth (e.g., compare Figure 1c of larger polymer with Figure 2b of smaller polymer).

Catalyst Activity. A major finding of this study is that more than half of all the resin support beads are inactive and do not contribute significantly to the growth of polymer; these are the inactive beads that stalled after the deformation time regime. Specifically, at 20 min, some beads showed high activity, visible as a large number of individual polymerization sites, while others showed lower activity (both a lower number of active sites and smaller growth at each site) or no activity (Figure 2a). All beads showed deformation, however. A representative sample of beads showing this interparticle heterogeneity is shown in Figure 2a, wherein one highly active bead is covered in polymer originating from multiple reactive loci, but four neighboring beads show little to no polymerization reactivity but do show the signature deformation that occurs in the presence of both monomer and solvent.

We considered three mechanistic explanations for this spatially heterogeneous polymerization activity (Figure 3): (1) The listed 0.5 mmol/g ruthenium loading of the commercial resin was erroneous; a much lower actual loading could account for the small number of active sites. (2) The

DOI: 10.1021/acscatal.5b00046
ACS Catal. 2015, 5, 2290−2295

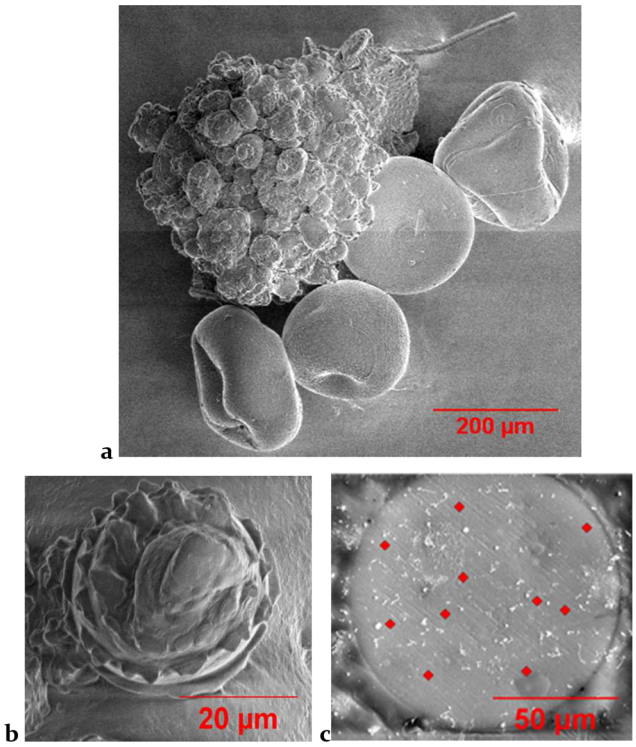

Figure 2. (a) Most beads are catalytically inactive. Between multiple beads at t = 20 min; one bead is highly reactive, four show little or no reactivity. (b) Nascent polymer morphology arises from individual active loci: on one bead, a single hemispherical polymer growth on one bead at high magnification, showing the regular repeating features on the micrometer and submicrometer scale. (c) EDS measurements on the cross-sectioned interior of a catalyst bead; measurement locations in the bead interior are marked with red diamonds. Regions were selected at random and have no distinguishing features.

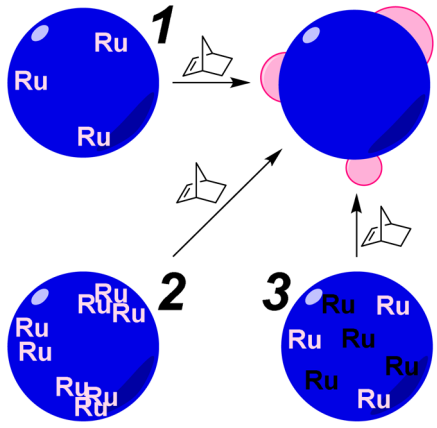

Figure 3. Three mechanistic possibilities for spatially nonuniform polymerization. (1) The manufacturer's stated loading was higher than the actual loading of catalyst throughout the support. (2) The catalyst was loaded only at specific sites throughout the support rather than uniformly. (3) The catalyst was uniformly loaded throughout the support, but only specific sites were active during catalysis.

catalyst was concentrated in a small number of locations within the support. This could explain why polymerization occurred at a countable number of locations. (3) A small number of ruthenium centers displayed high activity, while the majority displayed no activity or activity too low to detect by SEM.

Energy-Dispersive X-ray Spectroscopy. Single-particle microscopy techniques permitted differentiation among these three mechanistic possibilities. Examination of a flat, cross-sectioned slice of the interior of a catalyst bead with energy-dispersive X-ray spectroscopy (EDS) at multiple random measurement locations established that the ruthenium was uniformly loaded throughout the beads rather than localized at specific sites. With 10 measured locations, the concentration of Ru was 5.3 ± 0.3 wt % (Figure 2c). Both this small standard deviation and average loading are consistent with the listed loading of the commercial sample and with uniform loading at each measurement location. Thus, the ruthenium was distributed more uniformly throughout the support than was the catalytic reactivity.

PIXE elemental analysis of an ensemble of beads indicated a Ru concentration of 2.36 ± 0.02 wt %. The origin of the discrepancy between ruthenium loadings measured by PIXE and by EDS is unclear; however, both measurements indicate a similar order of magnitude for the ruthenium loading.

These data revealed that the ensemble rate of polymerization came from a small number of active ruthenium sites, whereas the majority of ruthenium did not contribute significantly to the measured ensemble rate (mechanistic option 3, Figure 3). These active sites could be individual ruthenium complexes, or they could be clusters of neighboring sites that become mutually activated as the growing polymer deforms the material and exposes additional ruthenium complexes to monomer, similar to how the hydraulic force of the growing polypropylene in the polymerization of propene by silica-supported metallocene catalysts cracks the rigid silica support and exposes neighboring catalyst centers to monomer and thus generates additional neighboring active sites.[1]

We also considered the possibility that the catalyst itself could be poorly initiating chemically, leading to catalysis originating from a small number of complexes. This suggestion has been raised as part of a long-standing debate on distribution of initiation rates for Grubbs–Hoveyda catalysts,[21−25] the distribution of which is obscured by traditional ensemble measurements. While providing an early picture of non-ensemble-averaged reactivity in this system, the current data remain insufficient to identify if the overall distribution is purely from a physical effect of the support or if it also includes this debated chemical component. The primary measurement challenge that remains in this supported system is the deconvolution of the physical and chemical effects. The nonzero contribution of physical effects were confirmed through later experiments that probed the effect mechanical bead deformation on reaction yields (vida supra).

In Operando Microscopy. Although SEM provided exceptional spatial resolution, it required removal of samples from the reaction vessel and subsequent drying, raising the possibility of artifacts. We therefore next examined if the spatial reactivity heterogeneity was also present under reaction conditions in the presence of solvent and monomer by using in operando optical microscopy. This in operando method had the advantage of following the behavior of the catalyst system through time without removal of the sample from the reaction vessel, albeit with the disadvantage of decreased spatial resolution compared to SEM.

In this in operando experiment, the catalyst beads were loaded into a modified reaction vial with a glass coverslip bottom, permitting imaging of the reaction by transmitted light microscopy. Toluene, a reported solvent[30] for efficient olefin

DOI: 10.1021/acscatal.5b00046
ACS Catal. 2015, 5, 2290−2295

metathesis, was selected to allow for easier optical imaging and also to examine if the catalytic spatial reactivity heterogeneity was present in this second solvent, as well.

Images were obtained first at t = 0 min and then continuously at video rate upon addition of solvent and monomer. Polymer growth in real time on individual beads could be detected as light gray translucent regions growing on dark black beads. Figure 4 shows a representative image of a

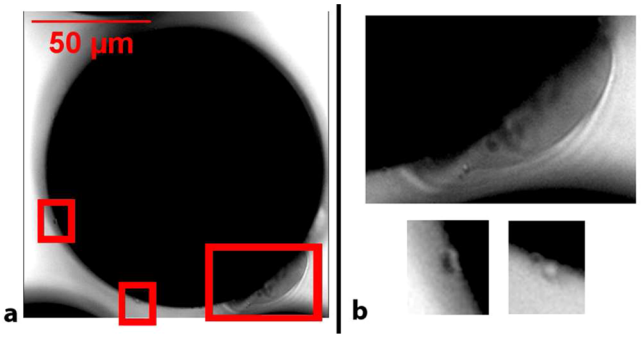

Figure 4. (a) Representative in operando optical microscopy image showing highly active and less active polymerization regions on the same black resin bead at t = 10 min. Polymer is visible as light gray translucent regions. (b) Three expansions corresponding to the three red boxed-in regions of the image on the left.

bead obtained with optical microscopy at t = 10 min. The polymer growth was not spherically uniform on these beads, but instead occurred at specific positions on the surface. The spatial reactivity distribution observed during in operando experiments therefore mirrored that observed previously by SEM.

Furthermore, over half of the beads did not show detectable polymer growth at 20 min by optical microscopy. Specifically, as measured over nine experiments with a total set size of 130 beads (averaging 14.4 beads per observation), 28 ± 8% of the beads showed observable polymerization catalysis at t = 20 min. The remainder of the beads, which appeared as black spheres without the visible growth regions (see SI for example; Figure S1), correspond to the less active (or inactive) beads detected by SEM (Figure 2a). Thus, the interparticle reactivity heterogeneity observed in DCE also was retained in toluene and under reaction conditions.

Concrete Suggestion for Improved Catalyst Efficiency. The previously discussed EDS data revealed an indiscriminate manufacturing process wherein the molecular ruthenium complexes were located uniformly throughout the support bead rather than only on its surface. This location data suggested that the challenge is to increase the number of sites becoming active to increase the catalytic efficiency, rather than increase the rate of polymerization from already active sites.

We hypothesized that mechanically pressing the catalyst beads prior to the catalytic reaction could result in faster entry into the third time regime of polymerization by "pre-deforming" the beads such that the 5 min induction/deformation period would be diminished; this process could generate a greater surface area that would expose more catalytic centers to monomer because the ruthenium complexes were evenly distributed throughout the beads.

Mechanical pressing created fissures in the beads, but otherwise left the beads mostly intact (Figure 5). These pressed beads displayed substantially higher catalytic efficiency

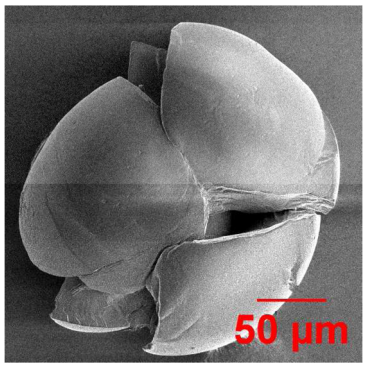

Figure 5. SEM micrograph of a mechanically pressed bead, showing fissures in support. The support retains a similar size and does not fragment into significantly smaller pieces.

in ensemble studies (Figure 6), as measured by polymer conversion per unit of time via ^{1}H NMR spectroscopy. The

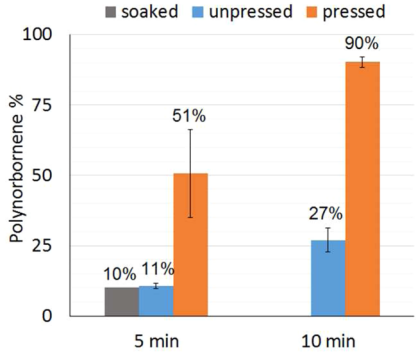

Figure 6. Increase in polynorbornene yield with pressed support beads (orange) compared with unpressed support beads as received from manufacturer (blue) measured via ^{1}H NMR spectroscopy relative to an internal standard. Control reaction with presoaking shows no similar increase (gray), consistent with heterogeneous catalysis rather than homogeneous catalysis by leached ruthenium.

comparison at 5 min shows a 5-fold increase in polynorbornene conversion (11 ± 1% unpressed, 51 ± 16% pressed), and at 10 min shows a 3-fold increase (27 ± 4% unpressed, 90 ± 2% pressed). These results demonstrate a strategy for successful catalyst improvement that retains the original desired properties/size range of the commercial supported catalyst; this strategy was derived from knowledge of the stages of the reaction and of the location of the ruthenium obtained by single-particle microscopy studies.

Control Reactions. To probe if the active catalysts in this system were, indeed, heterogeneous supported molecular ruthenium complexes or if they were homogeneous ruthenium complexes that had leached into solution, a series of control experiments were performed.

A first control experiment with presoaking the intact support was performed. Specifically, the support was presoaked for 20 min in the reaction solvent in the absence of norbornene, then norbornene was added. This system generated the same conversion to polynorbornene at 5 min (10%; gray bar, Figure 6) as was generated without the presoak (11 ± 1%, blue bar). Thus, the presoak, which would provide additional time for leaching, did not result in additional conversion to polymer. When taken together with the observation of polymers attached to the support by both SEM and optical microscopy, this set of

DOI: 10.1021/acscatal.5b00046
ACS Catal. 2015, 5, 2290−2295

experiments is consistent with the catalytic activity coming from the supported complex rather than leached molecular species in solution.

Further, this first control experiment established that the swelling of resin in DCE was insufficient to increase the generation of polynorbornene. These beads that soaked in solvent for 20 min in the absence of norbornene showed swelling, as detected by a larger bead diameter (but no deformation or dimpling) by SEM (Figure 1d). We considered the possibility that this swelling would be an alternative route to increasing the effective surface area of this supported catalyst; however, in this system, no such rate increase was correlated to the swelling, and the presoaked beads generated polynorbornene in conversion similar to those beads that were not presoaked. Thus, in this system, mechanical pressing provided the specific successful strategy for increasing the catalytic efficiency.

A second control experiment wherein the soaking solvent was removed from the beads via pipet after 10 min of soaking was examined. This process produced a sample of clear soaking liquid without any visible beads; however, pieces of supported catalyst smaller than visible detection may have remained, especially in the pressed-bead system (although most pressed beads retained similar sizes). After separation of the soaking solvent and the beads, the soaking solvent was added to norbornene monomer. The same experiment was conducted using the pressed beads to probe if pressing the beads may have resulted in enhanced ruthenium leaching into solution that was responsible for the increase in conversion observed upon pressing. The ^{1}H NMR spectroscopy yields of polynorbornene using the intact and pressed bead soaking solvents were 2.1 ± 0.3% and 5.0 ± 0.6%, respectively. These data indicated an upper limit to a homogeneous catalysis component of 2% out of the total intact bead 11% polymer yield and 5% out of the total pressed bead polymer yield of 51%.

CONCLUSION

The observations from SEM, EDS, and optical microscopy highlight the starkly contrasting pictures of reactivity available from ensemble-averaged data and from single-bead nonaveraged data in this catalytic system: The ensemble-averaged data gives the appearance of an efficient catalyst system that generates polymer in full conversion in about an hour at ambient temperature, whereas in contrast, the single-bead, nonaveraged data available from microscopy techniques provides evidence of an inefficient catalyst system wherein the majority of molecular ruthenium complexes do not contribute to overall catalytic reactivity. This revised picture of reactivity indicates a substantial potential for increased catalytic efficiency in this commercial system, which was partially tapped by predeforming the beads. Similar potentials for increased catalytic efficiency are likely also present in other catalytic systems that are currently described by ensemble data.[5]

ASSOCIATED CONTENT

Supporting Information

The following file is available free of charge on the ACS Publications website at DOI: 10.1021/acscatal.5b00046.

Synthetic methods, experimental protocols, data analysis, and enlarged microscopy images (PDF)

AUTHOR INFORMATION

Corresponding Author

*E-mail: blums@uci.edu.

Notes

The authors declare no competing financial interest.

ACKNOWLEDGMENTS

We thank the U.S. Department of Energy, Office of Basic Energy Sciences (DE-FG02-08ER15994) and the Alexander von Humboldt Foundation for funding. SEM and EDS were performed at the Laboratory for Electron and X-ray Instrumentation (LEXI) at UC Irvine using instrumentation funded in part by the National Science Foundation Center for Chemistry at the Space-Time Limit (CHE-082913). We thank Mr. Amirhossein Khalajhedayati for assistance with EDS preparation and measurements.

REFERENCES

(1) Fink, G.; Steinmetz, B.; Zechlin, J.; Przybyla, C.; Tesche, B. *Chem. Rev.* **2000**, *100*, 1377−1390.
(2) Buchmeiser, M. R. *Chem. Rev.* **2009**, *109*, 303−321.
(3) Parlett, C. M. A.; Bruce, D. W.; Hondow, N. S.; Lee, A. F.; Wilson, K. *ACS Catal.* **2011**, *1*, 636−640.
(4) Goretzki, R.; Fink, G.; Tesche, B.; Steinmetz, B.; Rieger, R.; Uzick, W. *J. Polym. Sci., Part A: Polym. Chem.* **1999**, *37*, 677−682.
(5) Buurmans, I. L. C.; Weckhuysen, B. M. *Nat. Chem.* **2012**, *4*, 873−886.
(6) De Smit, E.; Swart, I.; Creemer, J. F.; Karunakaran, C.; Bertwistel, D.; Zandbergen, H. W.; de Groot, F. M. F.; Weckhuysen, B. M. *Angew. Chem., Int. Ed.* **2009**, *48*, 3632−3636.
(7) Kox, M. H. F.; Stavitski, E.; Groen, J. C.; Pérez-Ramíre, J.; Kapteijn, F.; Weckhuysen, B. M. *Chem.—Eur. J.* **2008**, *14*, 1718−1725.
(8) Roeffaers, M. B. J.; Sels, B. F.; Uji-i, H.; De Schryver, F. C.; Jacobs, P. A.; De Vos, D. E.; Hofkens, J. *Nature* **2006**, *439*, 572−575.
(9) De Cremer, G.; Bartholomeeusen, E.; Pescarmona, P. P.; Lin, K.; De Vos, D. E.; Hofkens, J.; Roeffaers, M. B. J.; Sels, B. F. *Catal. Today* **2010**, *157*, 236−242.
(10) Fast, A.; Esfandiari, N. M.; Blum, S. A. *ACS Catal.* **2013**, *3*, 2150−2153.
(11) Hensle, E. M.; Blum, S. A. *J. Am. Chem. Soc.* **2013**, *135*, 12324−12328.
(12) Esfandiari, N. M.; Blum, S. A. *J. Am. Chem. Soc.* **2011**, *133*, 18145−18147.
(13) Cordes, T.; Blum, S. A. *Nat. Chem.* **2013**, *5*, 993−999.
(14) Blum, S. A. *Phys. Chem. Chem. Phys.* **2014**, *16*, 16333−16339.
(15) Esfandiari, N. M.; Wang, Y.; Bass, J. Y.; Blum, S. A. *Inorg. Chem.* **2011**, *50*, 9201−9203.
(16) Zhou, X.; Choudhary, E.; Andoy, N. M.; Zou, N.; Chen, P. *ACS Catal.* **2013**, *3*, 1448−1453.
(17) Andoy, N. M.; Zhou, X.; Choudhary, E.; Shen, H.; Chen, P. *J. Am. Chem. Soc.* **2013**, *135*, 1845−1852.
(18) Chen, P.; Zhou, X.; Andoy, N. M.; Han, K.-S.; Choudhary, E.; Zou, N.; Chen, G.; Shen, H. *Chem. Soc. Rev.* **2014**, *43*, 1107−1117.
(19) Flier, B. M. I.; Baier, M.; Huber, J.; Müllen, K.; Mecking, S.; Zumbusch, A.; Wöll, D. *Phys. Chem. Chem. Phys.* **2011**, *13*, 1770−1775.
(20) Ohm, R.; Stein, C. In *Encyclopedia of Chemical Technology*, 3rd ed.; Grayson, M., Ed.; Wiley-Interscience: New York, 1982.
(21) Vorfalt, T.; Wannowius, K.-J.; Thiel, V.; Plenio, H. *Chem.—Eur. J.* **2010**, *16*, 12312−12315.
(22) Gessler, S.; Randl, S.; Blechert, S. *Tetrahedron Lett.* **2000**, *41*, 9973−9976.
(23) Thiel, V.; Hendann, M.; Wannowius, K.-J.; Plenio, H. *J. Am. Chem. Soc.* **2012**, *134*, 1104−1114.
(24) Núñez-Zarur, F.; Solans-Monfort, X.; Pleixats, R.; Rodríguez-Santiago, L.; Sodupe, M. *Chem.—Eur. J.* **2013**, *19*, 14553−14565.

DOI: 10.1021/acscatal.5b00046
ACS Catal. 2015, 5, 2290−2295

(25) Bates, J. M.; Lummiss, J. A. M.; Bailey, G. A.; Fogg, D. E. *ACS Catal.* **2014**, *4*, 2387−2394.
(26) For examples of catalytic reactivity distributions attributed to physical/diffusion heterogeneities, see refs 5 and 7. For examples of catalytic reactivity distributions attributed to different chemical species/chemical environments, see refs 16, 17, 27, 28, and 29.
(27) Zhong, L.; Lee, M.-Y.; Liu, Z.; Wanglee, Y.-J.; Lui, B.; Scott, S. L. *J. Catal.* **2012**, *293*, 1−12.
(28) Tominaga, H.; Kiyoshi, M.; Nagai, M. *Chem. Eng. Sci.* **2007**, *62*, 5368−5373.
(29) Barabanov, A. A.; Bukatov, G. D.; Zakharov, V. A.; Semikolenova, N. V.; Mikenas, T. B.; Echevskaja, L. G.; Matsko, M. A. *Macromol. Chem. Phys.* **2006**, *207*, 1368−1375.
(30) Bielawski, C. W.; Benite, D.; Morita, T.; Grubbs, R. H. *Macromolecules* **2001**, *34*, 8610−8618.
(31) Chung, C. K.; Grubbs, R. H. *Org. Lett.* **2008**, *10*, 2693−2696.
(32) De Clerq, B.; Smellinckx, T.; Hugelier, C.; Maes, N.; Verpoort, F. *Appl. Spectrosc.* **2001**, *55*, 1564−1567.

DOI: 10.1021/acscatal.5b00046
ACS Catal. 2015, 5, 2290−2295